

Synthesis, Spectroscopic, Thermal, Free Radical Scavenging Ability, and Antitumor Activity Studies of Cobalt(II) Metformin Complex¹

Moamen S. Refat^{a,b} and Mohamed I. Kobeasy^{a,c}

^a Department of Chemistry, Faculty of Science, Taif University, 888 Taif, Kingdom Saudi Arabia
e-mail: msrefat@yahoo.com

^b Department of Chemistry, Faculty of Science, Port Said University, Port Said, Egypt

^c Department of Biochemistry, Faculty of Agriculture, Cairo University, Egypt

Received March 10, 2014

Abstract—New $[\text{Co}(\text{Mfn}\cdot\text{HCl})_2(\text{NO}_3)_2] \cdot 6\text{H}_2\text{O}$ complex has been synthesized and characterized using micro-analytical, molar conductance, spectroscopic (IR and UV-Vis), effective magnetic moment, and thermal analyses. The infrared spectroscopic results data received from the comparison between free $\text{Mfn}\cdot\text{HCl}$ ligand and its cobalt(II) complex proved that Metformin forms complex with cobalt(II) ions as a bidentate ligand through its two imino groups. The antioxidant activity of the $\text{Mfn}\cdot\text{HCl}$ and $\text{Co(II)}-2\text{Mfn}\cdot\text{HCl}$ complex were evaluated by using 1,1-diphenyl-2-picryl-hydrazyl (DPPH) radical scavenging method. Antitumor activity for $\text{Mfn}\cdot\text{HCl}$ ligand and its cobalt(II) complex was determined using Ehrlich Ascites carcinoma cell (EACC) line. It has been shown that the $\text{Co(II)}-\text{Mfn}\cdot\text{HCl}$ complex is much more effective as free radical scavenger and has higher antitumor activity than the free $\text{Mfn}\cdot\text{HCl}$ ligand.

Keywords: metformin hydrochloride, cobalt(II) complex, anti-tumour activity, spectroscopic, thermal

DOI: 10.1134/S1070363214040288

INTRODUCTION

Metformin (Fig. 1) is a moderately strong base and binds with many transition metals, especially Cu(II), Ni(II), and Pt(II) [1], due to the presence of the two imine groups in cis position, acting as a chelating agent. Metformin coordinates to the silicon atom in a neutral as well as a deprotonated form to yield two different types of complexes [2]. Complexes of metformin with Rh(III) [3], Ir(III) [4], Os(II) and Os(III) [5], Tc(V), and Re(V) [6] have also been studied.

With 2,6-pyridinedicarboxylic acid metformin forms complex with Pd(II), promising as an insulin-mimic compound [7]. Complexes of Cu(II), Ni(II) [8], Zn(II) [9] have shown significant increase in hypoglycemic activity when compared to pure metformin. Recently, metformin complexes of Mn(II), Fe(III), Ni(II), Cu(II), Zn(II), Cd(II), Mg(II), Sr(II), Ba(II), and Au(III) were synthesized and characterized as diabetic drug model agents [10].

Metformin is regularly used for the treatment of type 2 diabetes, particularly in overweight and obese people [11]. It inhibits gluconeogenesis in liver and increases glucose uptake by peripheral tissues through stimulation of the intracellular enzyme AMP activated protein kinase (AMPK) [12]. In addition to its antidiabetic properties, metformin has also been shown to inhibit in vitro growth of various types of cancer cells, such as breast cancer, prostate cancer and glioma cells as well as tumourigenesis and tumour progression in vivo [13]. Moreover, population studies have suggested that in diabetic patients metformin decreases the incidence of cancer and cancer-related mortality, while a recent report showed that metformin improves the response to chemotherapy in diabetic patients with breast cancer.

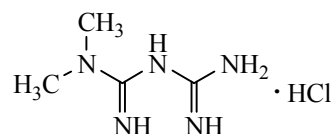


Fig. 1. Metformin hydrochloride ($\text{Mfn}\cdot\text{HCl}$).

¹ The text was submitted by the authors in English.

Transition metal ions are reported to play an important role in different enzymatic and physiological reactions. They take a part in the initiation of free radical processes [14] and the biological activity of an organic ligand can be increased when co-coordinated or mixed with suitable metal ion, because of its ability to act as a free radical acceptor [15]. Cobalt(II) is an element of biological interest that acts as metal cofactor of the coenzyme B12 and vitamin B12. It is very essential for health, keeps the metabolic system very strong, and helps to make body healthier by protecting against bacteria and viruses [16]. From pharmacological point of view, cobalt complexes are noted for their significant biological properties, namely antioxidant, antitumor, antibacterial and antifungal activities [17]. The aim of this paper was synthesis and spectroscopic characterization of cobalt(II)–Mfn · HCl complex as a prospective free radical scavenger and antitumor agent.

EXPERIMENTAL

All chemicals, solvents, cobalt(II) nitrate hexahydrate were commercially available from BDH and were used without further purification. The pure grade Metformin hydrochloride was received as a gift sample from Egyptian International Pharmaceutical Industrial Company (EIPICO).

IR spectra were recorded on a Bruker IR spectrophotometer in the range of 400–4000 cm^{-1} , at Taif University. Electronic spectrum of the Co(II) complex was measured in DMSO with concentration of 1×10^{-3} M, in the range 200–1100 nm using an Unicam UV-Vis spectrometer. X-ray diffraction (XRD) patterns of the samples were recorded on a X Pert Philips X-ray diffractometer. All the diffraction patterns were obtained by using $\text{CuK}_{\alpha 1}$ radiation, with a graphite monochromator at 0.02 deg/min scanning rate. Carbon, hydrogen and nitrogen analysis have been carried out on a Vario EL Fab. CHNS. The amount of water and the metal content percentage were determined by gravimetric analysis method. The molar conductance of 10^{-3} M solutions in DMF were measured on a HACH conductivity meter. All the measurements were taken at room temperature for freshly prepared solutions. Differential thermal analysis (DTA) and thermogravimetric analysis (TGA) experiments were conducted using Shimadzu DTA-50 and Shimadzu TGA-50H thermal analyzers, respectively. All experiments were performed using a single loose top loading platinum sample pan under nitrogen

atmosphere at a flow rate of 30 mL/min and a $10^\circ\text{C}/\text{min}$ heating rate for the temperature range 25–800°C. The mass susceptibility (X_g) of the cobalt(II) complex was measured at room temperature using Gouy's method on a magnetic susceptibility balance from Johnson Metthey and Sherwood. The effective magnetic moment (μ_{eff}) value was obtained using the following Eqs. (1), (2), and (3) [18].

$$X_g = \frac{C_{\text{Bal}}L(R - R_0)}{10^9 M}, \quad (1)$$

where R_0 is a reading of empty tube, L is a sample length, cm, M is a sample mass, g, R is a reading for tube with sample, C_{Bal} is a balance calibration constant = 2.086.

$$X_M = X_g \times MWt. \quad (2)$$

The values of X_M as calculated from Eq. (2) are corrected for the diamagnetism of the ligand using Pascal's constants, and then applied in Curie's Eq. (3)

$$\mu_{\text{eff}} = 2.84 \sqrt{X_M \times T}, \quad (3)$$

where $T = t(^{\circ}\text{C}) + 273$.

Biological evaluations. *Antioxidant radical scavenging activity.* The antioxidant activity was determined based on the radical scavenging ability in reacting with stable DPPH free radical according to Biois [19]. All tests and analyses were done in triplicate and the results were averaged.

Antitumor activity. Female Swiss albino mice weighing 25–30 g were obtained from the Toxicology Department at Central Agricultural Pesticide Laboratory, Agriculture Research Center and were housed at constant temperature ($24 \pm 2^\circ\text{C}$) with alternating 12 h light and dark cycles and were fed on standard laboratory food along with water ad-libitum. Animal care and handling was according to the guidelines set by the World Health Organization and was approved from the committee for animal care at Toxicology Department at Central Agricultural Pesticide Laboratory, Agriculture Research Center.

The Ehrlich ascites carcinoma cell (EACC) cell lines were obtained from the National Cancer Institute (NCI), Cairo University. The tumor cell line was maintained in female swiss albino mice through serial intraperitoneal inoculation at 7 or 8 days intervals in our laboratory in an ascites form.

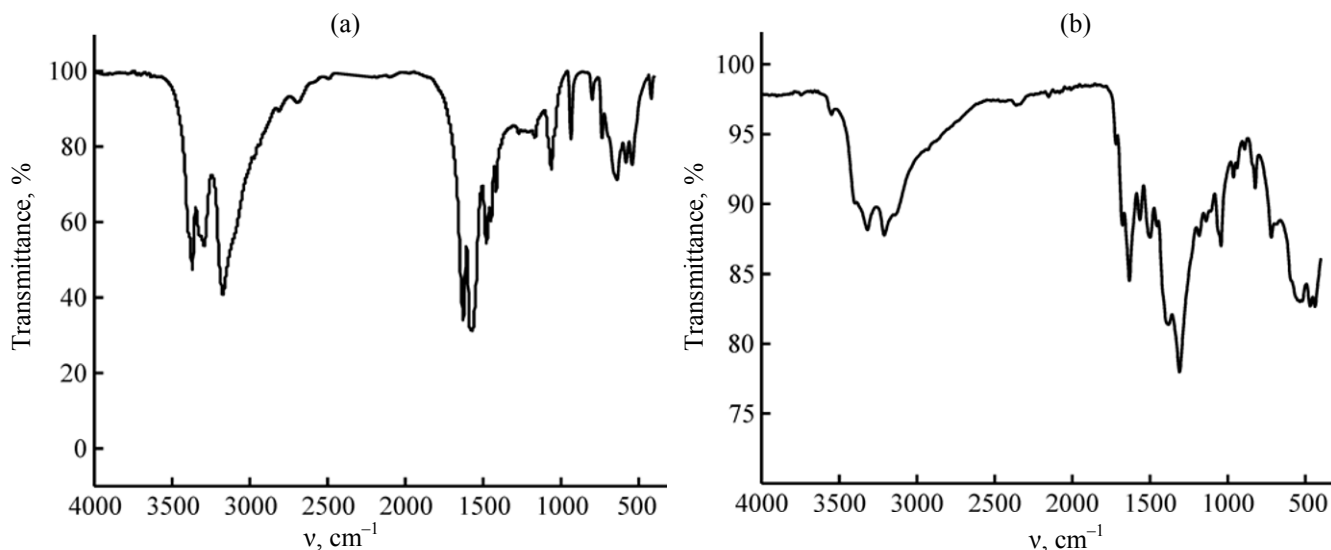


Fig. 2. IR spectra of (a) Mfn · HCl free ligand and (b) $[\text{Co}(\text{Mfn} \cdot \text{HCl})_2(\text{NO}_3)_2] \cdot 6\text{H}_2\text{O}$ complex.

All the experiments were done at the Biochemistry Department, Faculty of Agriculture, Cairo University. The *in vitro* cytotoxicity of the metformin HCl and metformin HCl cobalt(II) complex were tested against EACC cells by using trypan blue exclusion assay [20].

Co(II)–2Mfn · HCl. 2 mmol of metformin hydrochloride was dissolved in 25 mL of methanol then mixed with 25 mL of methanolic solution of 1 mmol $\text{Co}(\text{NO}_3)_2 \cdot 6\text{H}_2\text{O}$. A mixture was heated under reflux and continuous stirring at $\sim 70^\circ\text{C}$ for about 2 h. The mixture was left overnight until precipitate appeared. The precipitate obtained was filtered off and washed by diethyl ether and left over anhydrous calcium chloride to give desired complex in $\sim 60\%$ yield as turquoise crystals. Calculated, %: C 15.44; H 5.83; Co 9.47; N 27.01. $\text{C}_8\text{H}_{36}\text{Cl}_2\text{CoN}_{12}\text{O}_{12}$. Found, %: C 15.11; H 6.43; Co 8.93; N 26.32.

RESULTS AND DISCUSSION

Synthesized complex is soluble in dimethylsulfoxide and dimethylformamide, partially soluble in hot methanol and insoluble in water and some other organic solvents. The conductivity measured in DMF (at 10^{-3} M concentration) at room temperature, showed the molar conductance value of $48 \Omega^{-1} \text{cm}^2 \text{mol}^{-1}$, meaning that Co(II)–Mfn · HCl complex is of slightly electrolytic nature [22], that may be due to the contribution of the nitrate anions in the chelating skeleton.

The infrared absorption bands are one of the important tools of analyses used for determining the

mode of chelations. The most significant bands (Fig. 2) of Metformin HCl ligand can be classified into three groups: (1) NH vibrations of primary ($-\text{NH}_2$), secondary ($-\text{NH}$) and imino ($-\text{C}=\text{NH}$) groups; (2) C–N and C=N vibrational bands, and (3) C–H vibrations of the methyl groups. According to the three fundamental vibrational groups mentioned above, the Metformin HCl free ligand can be interpreted as follows: *N–H vibrations*: the N–H stretching of $\text{C}=\text{N}-\text{H}$ group occurs in the region of $3400\text{--}3100 \text{ cm}^{-1}$. Usually the frequency of this vibration decreases in the presence of the hydrogen bond [23]. The broad bands at 3370 cm^{-1} and those at 3294 and 3174 cm^{-1} have been assigned to N–H asymmetric and symmetric stretching vibrations, respectively [23]. The band at 1570 cm^{-1} has been assigned for NH_2 in the plane deformation vibrations [24]. The bands of the medium-to-weak intensities at 935 , 798 , and 735 cm^{-1} are due to N–H wagging. *C=N, C–N vibrations*: Metformin · HCl has strong absorption band at 1627 cm^{-1} due to C=N stretching vibration [24]. The medium-to-weak intensity bands in the IR spectra at 1271 , 1168 , and 1061 cm^{-1} have been assigned to C–N stretching vibrations of aliphatic amine compounds. Medium-to-weak intensity bands at 639 , 582 , 541 , and 419 cm^{-1} are due to CNC deformation vibrations [24]. *C–H vibrations*: CH stretching vibration of the aliphatic methyl group at $2975\text{--}2950 \text{ cm}^{-1}$ is for the asymmetric and that at $2885\text{--}2865 \text{ cm}^{-1}$ is for the symmetric CH_3 stretching vibrations [25]. In metformin HCl, the presence of nitrogen near methyl group reduces the symmetric CH_3

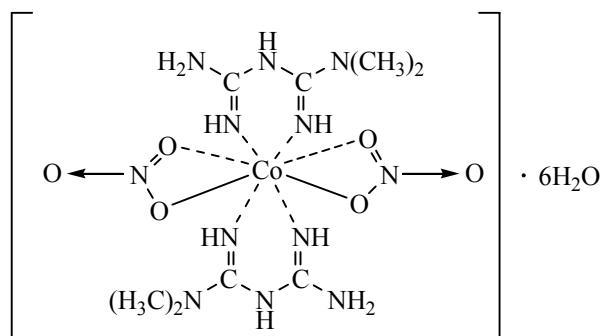


Fig. 3. Suggested structure for $[\text{Co}(\text{Mfn} \cdot \text{HCl})_2(\text{NO}_3)_2] \cdot 6\text{H}_2\text{O}$ complex.

stretching range to $2835\text{--}2815\text{ cm}^{-1}$ [26, 27]. Bands at 2965 , 2920 , and 2813 cm^{-1} are assigned to CH asymmetric and symmetric stretching vibrations of the methyl group. The methyl group has three deformation bands with medium intensity at 1479 , 1448 , and 1417 cm^{-1} [24]. The presence of the unshifted (but with significant intensity change) spectral bands of the imino group (--C=NH) in the Co(II) complex, indicates that metformin is coordinated to the metal ions through the nitrogen atom of the imino group without proton displacement. The second assumption is that, the stretching vibrational bands of $\nu_{\text{as}}(\text{NH})$ and $\nu_{\text{s}}(\text{NH})$ of (primary and secondary) amino group and that of the imino group were not greatly affected by chelation, showing non-participation of both --NH_2 and --NH , and the non-displacement of imino group (--C=NH) in the complexation process. The third evidence which denies the non-displacement of imino group, is the presence of the stretching vibration band of $\nu(\text{C=NH})$ almost unshifted and similar to that of the Metformin free ligand. In addition to that, very strong-to-medium bands observed at about 1389 and 1310 cm^{-1} indicate to the presence of coordinated nitrate group [28]. There is no definite borderline between lattice and coordinated water molecules, especially in the stretching of OH and bending $\delta(\text{H}_2\text{O})$ vibration. In addition to these interpretations the new bands at 469 and 438 cm^{-1} are assigned to the stretching vibration motions of $\nu(\text{M--N})$ [29].

Metformin hydrochloride free ligand has absorption in the ultraviolet (228 , 262 , and 284 nm) and visible (375 nm) regions and in some cases these bands extend over to higher wavelength region due to conjugation. But upon complexation with cobalt(II) ion, there is an interesting change in the electronic properties of the system. New bands due to charge transfer spectra from

metal to ligand (M–L) or ligand to metal (L–M) can be observed and this data can be processed to obtain information regarding the structure and geometry of the complexes [30]. UV-Vis peaks corresponding to the $\pi \rightarrow \pi^*$ transitions in the $\text{Mfn} \cdot \text{HCl}$ cobalt(II) complex was observed at 260 and 270 nm [31]. This transitions ($\pi \rightarrow \pi^*$) could be assigned to the aromaticity of the double bond. The peaks belonging to $n \rightarrow \pi^*$ transitions are recorded at wavelengths 370 nm [32]. This is most probably due to the $n \rightarrow \pi^*$ transitions of imine ($=\text{NH}$), primary (--NH_2), secondary (--NH), and tertiary [$\text{--N}(\text{CH}_3)_2$] amino groups. The transition in visible region located at 520 nm for cobalt(II) complex and can be attributed to the ligand-to-metal charge transfer bands LMCT from the electronic lone pairs of adjacent nitrogen coordinated to the cobalt(II) ions [33]. The electronic spectrum of the $\text{Mfn} \cdot \text{HCl}$ ligand exhibited maximum band at 375 nm , which could be assigned to the $n \rightarrow \pi^*$ transition of the imine ($=\text{NH}$), primary (--NH_2), and secondary (--NH) amino groups. This band shows a blue shift of the absorbance intensity in cobalt(II) complex. This clearly indicates the coordination of the imine nitrogen atom with the metal atom. The electronic spectrum of octahedral Co(II) complex has three types of transitions at 13404 , 17391 , and 21810 cm^{-1} due to ${}^4T_{1g}(\text{F}) \rightarrow {}^4T_{2g}(\text{F})$, ${}^4T_{1g}(\text{F}) \rightarrow {}^4A_{2g}(\text{F})$, and ${}^4T_{1g}(\text{F}) \rightarrow {}^4T_{2g}(\text{P})$ [34, 35], respectively. The octahedral geometry of Co(II) complex has a magnetic moments, number of unpaired electrons, corresponding to configuration and expected value as 5.60 BM , 3 , d_7 , and 4.56 , respectively. On the basis of the above, the suggested structure of the cobalt(II)– $\text{Mfn} \cdot \text{HCl}$ complex can be represented as in Fig. 3.

The homogeneity, surface morphology and chemical composition of $\text{Mfn} \cdot \text{HCl}$ free ligand and Co(II) complex were studied using SEM. The surface morphology of SEM micrograph reveals the well uniform nature of the $[\text{Co}(\text{Mfn} \cdot \text{HCl})_2(\text{NO}_3)_2] \cdot 6\text{H}_2\text{O}$ complex with variant grain sizes and shapes. Clearly, large grains are obtained with agglomerates. The distribution of the grain size is homogeneous. X-ray powder diffraction patterns in the range of $5^\circ < 2\theta < 80^\circ$ of the $\text{Mfn} \cdot \text{HCl}$ free ligand and Co(II) complex were done. The crystallite size could be estimated from XRD patterns by applying FWHM of the characteristic peaks using Deby–Scherrer equation (4) [36].

$$D = K\lambda/\beta \cos \theta, \quad (4)$$

where D is the particle size of the crystal gain, K is a constant (0.94 for Cu grid), λ is the X-ray wavelength

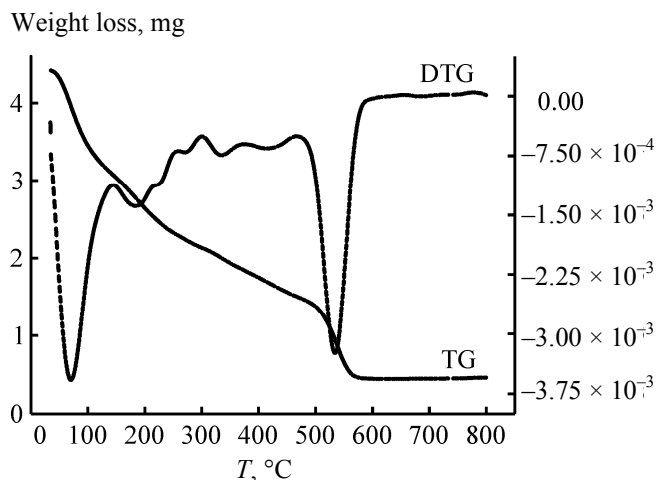


Fig. 4. TG and DTG curves of $[\text{Co}(\text{Mfn} \cdot \text{HCl})_2(\text{NO}_3)_2] \cdot 6\text{H}_2\text{O}$ complex.

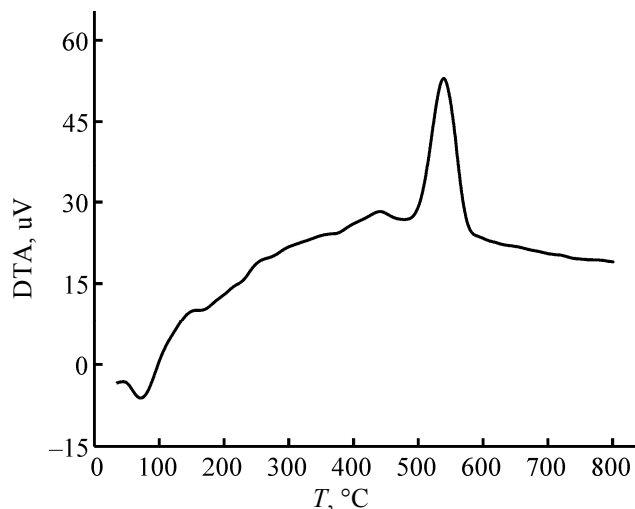


Fig. 5. DTA curve of $[\text{Co}(\text{Mfn} \cdot \text{HCl})_2(\text{NO}_3)_2] \cdot 6\text{H}_2\text{O}$ complex.

(1.5406 Å), θ is the Bragg diffraction angle and β is the integral peak width. The particle size was estimated according to the highest value of intensity compared with the other peaks. These data gave an impression that mean particle size is within nano scale range.

Thermal analysis. The thermal analysis of metformin hydrochloride free ligand [10] shows two main consecutive steps of mass loss at the temperature ranges of 181–410°C and 410–600°C.

The TG/DTG and DTA curves recorded for the $[\text{Co}(\text{Mfn} \cdot \text{HCl})_2(\text{NO}_3)_2] \cdot 6\text{H}_2\text{O}$ complex are given in Figs. 4 and 5. These curves, which characterize and compare the thermal decomposition behaviour of the $\text{Mfn} \cdot \text{HCl}$ ligand show five successive degradation steps at 30–150, 150–220, 220–375, 375–480, and 480–800°C.

The kinetic and thermodynamic parameters were determined using non-isothermal methods. The non-isothermal kinetic analysis for the thermal decomposition in this work was carried out by the application of the Coats–Redfern [37] and Horowitz–Metzger [38] methods. From the TGA curves (TG/DTG) recorded for the successive steps in the decomposition process of $\text{Mfn} \cdot \text{HCl}$ ligand and its

cobalt(II) complex, it was possible to determine the following characteristic thermal parameters for each reaction step as follows:

Initial point temperature of decomposition (T_i): the point at which DTG curve starts deviating from its base line. Final point temperature of decomposition (T_f): the point at which DTG curve returns to its base line. Peak temperature, i. e. temperature of maximum rate of mass loss (TD/TG): the point obtained from the intersection of tangents to the peak of DTG curve. Mass loss at the decomposition step (Δm): it is the amount of mass that extends from the point T_i up to the point T_f on the TG curve. The material released at each step of the decomposition is identified by attributing the mass loss (Δm) at a given step to the component of similar weight calculated from the molecular formula of the investigated compounds, comparing that with the literature for relevant compounds considering their temperature. This may assist in identification of the mechanism of reaction in the decomposition steps taking place in the complex under study. Activation energy (E^*) of the decomposition step: the integral method used is the Coats–Redfern equation [37] for reaction order $n \neq 1$, which when linearized for a correctly chosen n yields the activation energy from the slope:

$$\log \left[\frac{1 - (1 - \alpha)^{1-n}}{T^2(1-n)} \right] = \log \frac{ZR}{qE_a} \left[1 - \frac{2RT}{E_a} \right] - \frac{E_a}{2.303RT} \quad \text{for } n \neq 1,$$

$$\log \left[\frac{-\log(1 - \alpha)}{T^2} \right] = \log \frac{ZR}{qE_a} \left[1 - \frac{2RT}{E_a} \right] - \frac{E_a}{2.303RT} \quad \text{for } n = 1,$$

Table 1. Antioxidant activity (%) of metformin and metformin cobalt(II) complex against DPPH. Radical scavenging assay

Compound	Concentration, µg/mL				
	25	50	100	200	300
Mfn·HCl	11	7	23	29	41
Mfn·HCl–Co(II) complex	19	24	29	35	62
Butylated hydroxyanisole (BHA) (standard)	29	42	49	73	89

Table 2. Viability (%) of carcinoma cells treated with Metformin and Metformin cobalt(II) complex at different concentrations

$$\text{Cell viability (\%)} = \frac{(\text{number of viable cells}) \times 100}{\text{Total number of cells}}$$

Compound	Concentration, µg/mL				
	25	50	100	200	300
Mfn·HCl	91	88	85	72	68
Mfn·HCl–Co(II) complex	76	70	65	39	19
DMSO (control)	100	100	100	100	100

where α is a fraction of weight loss, T is a temperature (K), n is an order of reaction, Z is a pre-exponential factor, R is a molar gas constant, E_a is an activation energy and q is a heating rate. The activation energies (E_a) are calculated from the slopes of the best fit straight lines ($r \approx 1$) obtained when the plots of the Coats–Redfern equation [37] are used for the best values of reaction order (n). Order of reaction (n): it is the one for which a plot of the Coats–Redfern expression gives the best straight line among various trial values of n that are examined, i. e., by trial and error for various trial values of n , estimated by the Horowitz–Metzger method [38]. The thermodynamic parameters: entropy change (ΔS^*), enthalpy change (ΔH^*) and free energy of activation change (ΔG^*) were calculated using the following equations:

$$\Delta S^* = R[\ln(Zh/KT)], \quad (5)$$

$$\Delta H^* = E_a - RT_s, \quad (6)$$

$$\Delta G^* = \Delta H^* - T_s \Delta S^*, \quad (7)$$

where, Z , K , and h are the pre-exponential factor, Boltzman and Plank constants, respectively [39].

The negative ΔS^* values indicate that the activated complex has more ordered structure than the reactants and the reactions are slower than normal [40]. The positive values of ΔG^* indicate the non-spontaneous character for the reactions at the transition-state. The positive ΔH^* values show endothermic transition-state

reactions [41]. From the abnormal values of Z , the reactions of the complexes at the transition-state can be classified as a slow reaction [42]. The higher stability of the cobalt(II) complex than that of the Mfn·HCl ligand may be due to the formation of two stable 6-membered rings structures in the metal complexes [43] and the higher is the molecular symmetry the more stable is the molecule [44].

Biological evaluation. In vitro antioxidant activity. Antioxidant activity of Metformin hydrochloride and Metformin cobalt(II) complex were carried out by DPPH radical scavenging assay. This assay was used as a principle antioxidant as a fast test (H-donor method) and was used to determine the antioxidant activity by using a stable free radical α, α -diphenyl- β -picrylhydrazyl (DPPH) and is based on the measurement of the scavenging capacity of an antioxidant towards it. The odd electron of nitrogen atom in DPPH is reduced by receiving a hydrogen atom from antioxidants [45]. Results of inhibition test are presented in Table 1. The scavenging effects on the DPPH radical decreased in order of BHA > [Co(Mfn·HCl)₂(NO₃)₂]·6H₂O complex > metformin HCl which were 89, 62, and 41%, respectively. These results indicate that high antioxidant activity of [Co(Mfn·HCl)₂(NO₃)₂]·6H₂O complex may be due to metallic complexes such as, because cobalt and manganese are very effective inhibitors of lipid peroxidation and the inhibition mechanism of metallic-complex consists in

enhancing antiradical properties due to additional superoxide dismuting activity [47]. It is suggested that the increasing of the biological activity of an organic ligand can be caused by co-coordination with suitable metal ion, because of its ability to act as free radical acceptor [48]. On the other hand the antioxidant activity of $\text{Mfn} \cdot \text{HCl}$ may be in preventing reactive oxygen species (ROS) from activating B cell apoptotic pathways, decreasing insulin synthesis and contributing to insulin resistance [49]. High level of lipid peroxidation is accompanied by increasing the activities of superoxide dismutase (SOD) and glutathione peroxidase (Gpx) [50]. Catalyzing the dismutation of superoxide radical to hydrogen peroxide causes the increasing the activity of (SOD) and the levels of H_2O_2 which accompanied with oxidative damage following hydroxyl radical formation. Moreover, superoxide radical is reported to inhibit catalase (CAT) activity [51]. In this case Metformin exhibits antioxidant protective effect by decreasing the activities of SOD, Gpx, and TBARS level and increasing the CAT activity.

Antitumor activity. Results from tropan blue assay are presented in Table 2. It was shown that Metformin and its cobalt(II) complex compounds exhibited broad-spectrum antitumor activity, with $[\text{Co}(\text{Mfn} \cdot \text{HCl})_2(\text{NO}_3)_2] \cdot 6\text{H}_2\text{O}$ complex to have higher antitumor activity compared with Mfn free ligand. Antitumor activity of Metformin may be caused by its antioxidant effects thus it can play a role in cancer treatment and prevention by prevent cancer cells from using the mitochondria to grow and spread throughout the body [52]. Metformin helps to decrease cancer risk in diabetic patients treated with this drug by reducing mutagenesis induced by reactive oxygen species [53] and the mechanism for the reduction of cancer risk is as follows: (1) at the cellular level, Metformin induces cell-cycle arrest, autophagy, and cell death, depending on the cancer cell origin [54]. It also affects cancer cell metabolism and inhibits the activity of the mitochondrial complex in hepatocytes and cancer cells; (2) at the molecular level Metformin activates AMP-activated kinase (AMPK), a kinase regulated by liver kinase B1 (LKB1), a tumor suppressor gene. AMPK activation inhibits mTOR, which controls protein synthesis. Altogether, these observations suggest a direct action of Metformin on cancer cell proliferation [53]. Also the in vivo effects of Metformin may be direct and/or indirect, due to the associated decrease in insulin levels as decreased hyperglycemia. Indeed, insulin as well as insulin-like growth factor 1 (IGF-1) are key factors in promoting cancer development [55].

It is suggested that Metformin inhibits ROS production through the inhibition of the mitochondrial complex (the two main producers of ROS). This decrease of complex activity would reduce ROS production by reducing the electrons in the electron transport chain. Hence the antioxidant properties of Metformin could provide benefit against not only diabetes but cancer as well [52, 53]. On the other hand highly antitumor activity of Metformin cobalt(II) complex may be due to cobalt(II) complex enhanced lipid peroxidation and upregulation of other oxidative stress parameters. Co(II) ions can replace Mg^{2+} in enzymatic physiological enzyme reactions which strongly enhance DNA cleavage by topoisomerase [56], and cobalt complex binding with the histidine units of polypeptide chains of tumor cells. Moreover, cobalt complexes may catalyze auto-oxidation of ascorbic acid involving generation of superoxide radical, hydroxyl radical and H_2O_2 . Thus, cobalt complexes accumulated in malignant tissues should exhibit enhanced antitumor activity in cooperation with ascorbic acid [56]. In summary, Metformin exhibits antitumor activity by reducing ROS production through inhibition the mitochondrial complex I and III and mutagenesis, while antitumor activity of Metformin cobalt(II) complex is caused by enhancing lipid peroxidation and upregulation of other oxidative stress parameters or DNA intercalation or catalyze auto-oxidation of ascorbic acid.

REFERENCES

1. Zhu, M., Lu, L., Yang, P., and Jin, X., *Acta Crystallogr. E*, 2002, vol. 58, p. 217.
2. Meenu, P., *J. Phosphorus Sulfur Silicon*, 2012, vol. 187 (9), p. 1026.
3. Spacu, P. and Gheorghiu, C., *J. Less Common Met.*, 1968, vol. 15, p. 331.
4. Gheorghiu, C., *Z. Anorg. Allg. Chem.*, 1969, vol. 365, p. 91.
5. Spacu, P. and Gheorghiu, C., *J. Less Common Met.*, 1969, vol. 18, p. 117.
6. Marchi, A., Marvelli, L., Cattabriga, M., Rossi, R., Neves, M., Bertolasi, V., and Ferretti, V., *J. Chem. Soc. Dalton Trans.*, 1999, p. 1937.
7. Moghimi, A., Khavassi, H.R., Dashtestani, F., Kordestani, D., Ekram Jafari, A., Maddah, B., and Moosavi, S.M., *J. Mol. Struct.*, 2011, vol. 996, p. 38.
8. Rao, N.K. and Annapurna, M.M., *Research Papers*, 2007, vol. 3, p. 1.
9. Sandeep, R.N., Nirankar, N.M., Pratibha, P., Ashok, K., and Pitre, K.S., *Indian J. Exp. Biol.*, 1996, vol. 34, p. 81.
10. Al-Saif, F.A. and Refat, M.S., *J. Therm. Anal. Calorim.*, 2012, vol. 111(3), p. 2079.

11. Janjetovic, K., Vucicevic, I., Misirkic, M., Villmanovich, U., Tovilovic, G., Zogovic, S., Bum-basirevic, V., Trajkovic, V., and Trajkovic, L., *Eur. J. Pharmacology*, 2011, vol. 651, p. 41.
12. Correia, S., Carvalho, C., Cantos, M.S., Proenca, T., Nunes, E., Duarte, A.L., Monteiro, B., Seica, R., Oliveira, C.R., and Moreira, P.I., *Med. Chem.*, 2008, vol. 4, p. 358364.
13. Huang, X., Wullschleger, S., Shpiro, N., McGuire, V.A., Sakamoto, K., Woods, Y.L., McBurnie, W., Fleming, S., and Alessi, D.R., *Biochem. J.*, 2008, vol. 412, p. 211.
14. Bukhari, B.S., Memon, S., Mahroof Tahir, M., and Bhanger, M.I., *J. Mol. Struct.*, 2008, vol. 892, p. 39.
15. Moridani, M.Y., Pourahmad, J., Bui, H., Siraki, A., and Brien, P.J., *Free Radic. Biol. Med.*, 2003, vol. 34, p. 243.
16. Elson, M. and Hass, M.D., *Healthy with Nutrition: The Complete Guide to Diet and Nutrition Medicine*, Celestial Arts, 2006.
17. Ramachandran, E., Thomas, S.P., Poornima, P., Kalaivani, P., Prabhakaran, R., Padma, V.V., and Natarajan, K., *Eur. J. Med. Chem.*, 2012, vol. 50, p. 405.
18. Selwood, P.F., *Magnetochemistry*, 2nd ed., New York: Wiley Interscience, 1956.
19. Biois, M.S., *Nature*, 2000, vol. 26, p. 1199.
20. Bennett, J.M., Catovsky, D., Danniel, M.T., Galton, D.A.G., Graanlink, H.R., and Sultan, C., *British J. Hematology*, 1976, vol. 33, p. 451.
21. UmaDevi, P., Soloman, F.E., and Sharada, A.C., *Pharm. Biol.*, 1999, vol. 73, p. 231.
22. Refat, M.S., *Spectrochim Acta (A)*, 2007, vol. 68(5), p. 1393.
23. Bellamy, L.J., *The Infrared Spectra of Complex Molecules*, 3 ed., London: Chapman and Hall; 1975.
24. Socrates, G., *Infrared Characteristic Group Frequencies*, 1 ed., New York: Wiley, 1980.
25. Shanmugam, R. and Sathyanarayana, D.N., *Spectrochim Acta (A)*, 1984, vol. 40(8), p. 757.
26. Sharma, A., Gupta, V.P., and Virdi, A., *Indian J. Pure Appl. Phys.*, 2004, vol. 42(4), p. 251.
27. Dalton, F., Hill, R.D., and Meakins, G.D., *J. Chem. Soc.*, 1960, vol. 590, p. 2927.
28. Nakamoto, K., *Infrared and Raman Spectra of Inorganic and Coordination Compound*, New York: Wiley, 1978.
29. Ross, S.D., *Inorganic Infrared and Raman Spectra*, Mc Graw Hill, London, 1972.
30. Singh, H.L. and Varshney, A.K., *Bioinorg. Chem. Appl.*, 2006, vol. 2006, p. 1.
31. Ozturk, O.F., Sekerci, M., and Ozdemir, E., *Russ. J. Coord. Chem.*, 2005, vol. 31(9), p. 687.
32. Ozturk, O.F., Sekerci, M., and Ozdemir, E., *Russ. J. Gen. Chem.*, 2006, vol. 76, p. 33.
33. Allan, J.R., Baird, N.D., and Kassyk, A.L., *J. Therm. Anal.*, 1979, vol. 16(1), p. 79.
34. Ray, S., Konar, S., Jana, A., Jana, S., Patra, A., Chatterjee, S., Golen, J.A., Rheingold, A.L., Mandal, S.S., and Kar, S.K., *Polyhedron*, 2012, vol. 33 (1), p. 82.
35. Girasolo, M.A., Canfora, L., Sabatino, P., Schillaci, D., Foresti, E., Rubino, S., Ruisi, G., and Stocco, G., *J. Inorg. Biochem.*, 2012, vol. 106(1), p. 156.
36. Quan, C.X., Bin, L.H., and Bang, G.G., *Mater. Chem. Phys.*, 2005, vol. 91, p. 317.
37. Coats, W. and Redfern, J.P., *Nature*, 1964, vol. 201, p. 68.
38. Horowitz, H.H. and Metzger, G., *Anal. Chem.*, 1963, vol. 35, p. 1464.
39. Mahfouz, R.M., Monshi, M.A., Alshehri, S.M., El-Salam, N.A., and Zaid, A.M.A., *Synth. React. Inorg. Met.-Org. Chem.*, 2001, vol. 31(10), p. 1873.
40. Frost, A.A. and Pearson, R.G., *Kinetics and Mechanism*, New York: Wiley, 1961.
41. Hamada, M.M., Shallaby, A.H.M., El-Shafai, O., and El-Asmy, A.A., *Trans. Met. Chem.*, 2006, vol. 31, p. 522.
42. Sharma, P.K., Sen, A.K., and Dubey, S.N., *Indian J. Chem.*, 1994, vol. 6, p. 291.
43. El-Metwally, N. and El-Asmy, A.A., *J. Coord. Chem.*, 2006, vol. 59(14), p. 1591.
44. Xinquan, X. and Anbang, D., *Pure Appl. Chem.*, 1988, vol. 60(8), p. 1217.
45. Sagar, B., Kedare, R., and Singh, P., *J. Food Sci Technol.*, 2011, vol. 48(4), p. 412.
46. Shimada, K., Fujikama, K., Yahara, K., and Nakamura, T., *J. Agricultural Food Chem.*, 1992, vol. 40, p. 945.
47. Afanas'ev, I. B., Ostrakhovitch, E. A., Mikhal'chik, E.V., Ibragimova, G.A., and Korkina, L.G., *Biochem. Pharmacol.*, 2001, vol. 61, p. 677.
48. Hui-Lu, W., Jing-Kum, Y., Ying, B., Fei, J., Bin, L., and Fan, K., *Trans. Met. Chem.*, 2011, vol. 36(8), p. 819.
49. Simmons, R.A., *Free Radical Biol. Med.*, 2006, vol. 40, p. 917.
50. Robertson, R.P. and Harmon, J.S., *FEBS Lett.*, 2007, vol. 581, p. 3743.
51. Kono, Y. and Fridovich, I., *J. Biol. Chem.*, 1982, vol. 257, p. 5751.
52. Watson, J., *Open Biol.*, 2013, vol. 3, p. 1.
53. Bost, F., Ben-Sahra, I., and Tanti, J., *Cancer Prev. Res.*, 2012, vol. 5(4), p. 503.
54. Tomic, T., Botton, T., Cerezo, M., Robert, G., and Luciano, F., *Cell Death Dis.*, 2011, vol. 2, p. 199.
55. Gallagher, E. and Leroith, D., *Endocrinology*, 2011, vol. 152, p. 2546.
56. Jungwirth, U., Kowol, R.C., Keppler, B.K., Hartinger, G.C., Berger, W., and Heffeter, P., *Antioxid. Redox Signaling*, 2011, vol. 60, p. 1.